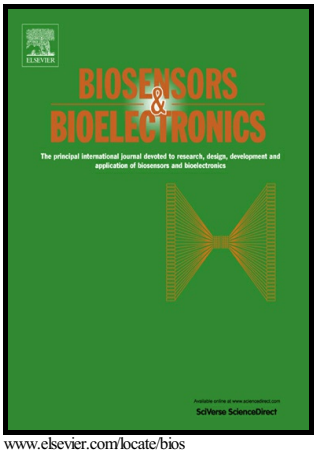

www.elsevier.com/locate/bios

A novel electrochemiluminescence biosensor for the detection of microRNAs based on a DNA functionalized nitrogen doped carbon quantum dots as signal enhancers

Qiao Liu, Cheng Ma, Xing-Pei Liu, Yu-Pin Wei, Chang-Jie Mao, Jun-Jie Zhu

PII: S0956-5663(17)30115-X
DOI: http://dx.doi.org/10.1016/j.bios.2017.02.027
Reference: BIOS9561

To appear in: *Biosensors and Bioelectronic*

Received date: 7 September 2016
Revised date: 15 February 2017
Accepted date: 16 February 2017

Cite this article as: Qiao Liu, Cheng Ma, Xing-Pei Liu, Yu-Pin Wei, Chang-Jie Mao and Jun-Jie Zhu, A novel electrochemiluminescence biosensor for the detection of microRNAs based on a DNA functionalized nitrogen doped carbon quantum dots as signal enhancers, *Biosensors and Bioelectronic* http://dx.doi.org/10.1016/j.bios.2017.02.027

A novel electrochemiluminescence biosensor for the detection of microRNAs based on a DNA functionalized nitrogen doped carbon quantum dots as signal enhancers

Qiao Liu [a,b], Cheng Ma[b], Xing-Pei Liu [a], Yu-Pin Wei [a], Chang-Jie Mao [a,*], Jun-Jie Zhu [b,**]

[a] School of Chemistry and Chemical Engineering, Anhui University, Hefei 230039, P. R. China.

[b] State Key Laboratory of Analytical Chemistry for Life Science, School of Chemistry& Chemical Engineering, Nanjing University, Nanjing 210093, P. R. China

maochangjie@sina.com
jjzhu@nju.edu.cn

[*]Corresponding author. Tel./fax: +86 551 6386 1260.

[**]Corresponding author. Tel./fax: +86 25 85866396.

ABSTRACT

An ultrasensitive electrochemiluminescence (ECL) biosensor for the detection of microRNA was developed based on nicking enzymes Nb.BbvCI mediated signal amplification (NESA). First, the hairpin probe1-QDs with assistant probe and microRNA (miRNA) formed Y junction structure which was cleaved with the addition of nicking enzymes Nb.BbvCI to release miRNA and assistant probe. Subsequently, the released

miRNA and assistant probe can initiate the next recycling process. The generation of numerous intermediate sequences nitrogen doped carbon quantum dots-DNA (N-CQDs-DNA) can further hybridize with hairpin probe2 immobilized on GO/Au composite modified electrode surface, the initial ECL intensity was enhanced. The ECL intensity would increase with increasing concentration of the target miRNA, and the sensitivity of biosensor would be promoted because of the efficient signal amplification of the target induced cycling reaction. The novel designed biosensor provided a highly sensitive and selective detection of miRNA-21 from 10 aM to10^4 fM with a relatively low detection limit of 10 aM. Thus, our strategy has a potential application in the clinical diagnosis.

Keywords:

Nitrogen doped carbon quantum dots; nicking enzymes; miRNA-21; electrochemiluminescence biosensor; signal amplification

1. Introduction

Carbon quantum dots (CQDs) have attracted attention because of their particular properties and functions regarding low toxicity (Mueller et al., 2010), good biocompatibility (Pan et al., 2010), excellent light stability (Yan et al., 2010), and sturdy chemical inertness (Han et al., 2015). However, insufficient optical characteristics and the surface chemical structure of CQDs limit the range of their practical applications. Therefore, to expand the range of applications, research has focused on CQDs surface modifications with different functionalities (Lim et al., 2015; Tetsuka et al., 2012). Doping is an excellent method to modify the properties of CQDs (Wu et al., 2013). Nitrogen-doped CQDs (N-CQDs) usually have a positive surface potential stemming from nitrogenous organic precursors. The amino groups on the surface can not only improve their fluorescence, but also facilitate subsequent modification and application (Yu et al., 2013). Because of their excellent luminous properties, light stability, and photoelectric physical properties, they have been widely used in the fields of biomedical

fluorescent tags (Wang et al., 2016; Jiang et al., 2015), ion detection (Zhang et al., 2014; Li et al., 2013), and photocatalysts (Martinsa et al., 2016). The inherent virtues of N-CQDs stimulate exploration into their possible applications in electrochemiluminescence (ECL), since they are superior to the traditional inorganic nanomaterials because of their low cost, easy operation, nontoxic nature, and high detection sensitivity. Moreover, although some N-CQDs have been shown to possess ECL emission properties, there are several challenges related to their low water solubility, defects of complex operating processes, and low or unstable ECL signal for N-CQDs (Kumar et al., 2016; Xiong et al., 2016).

MicroRNAs (miRNAs) are a class of small (19-25 nucleotides) noncoding RNA molecules found in eukaryotic cells that play a critical role in gene expression in most eukaryotic organisms from plants to animals (Wienholds et al., 2005; Bernstein et al., 2001). They are post-transcriptional regulators that cause translational repression or target degradation and gene silencing via binding to complementary sequences on target mRNAs (Bartel et al., 2009). Increasing evidence suggests that aberrant repression of miRNAs is associated with many diseases (Huang et al., 2014), including cancer (Kosaka et al., 2010; Volinia et al., 2006) and neurodegeneration (Hébert et al., 2007). The expression profile of miRNAs can thus serve as a biomarker for the diagnosis and treatment of cancer and other diseases, underscoring the need to develop highly sensitive, selective, and simple methods to detect miRNAs. ECL has attracted great interest in analytical methodology because of its unique advantages of low background signal, simplified optical setup, and high sensitivity (Hu et al., 2010; Miao et al., 2008). The ECL properties of quantum dots have attracted attention because of their excellent optical and electrochemical properties (Hesari et al., 2015). However, most quantum dots used in ECL studies are characterized by inherent toxicity due to the existence of toxic metal ions (e.g., cadmium), which limits their applications in bioassays (Hu et al., 2013). To improve the ECL intensity and biocompatibility, graphene oxide (GO) have been use

as efficient carriers due to their lager specific surface area and excellent mechanical strength. Moreover, gold nanoparticles (AuNPs) is an excellent sensing material due to its high sensitivities and excellent reliability. GO/Au nanocompsite can greatly improve the sensitivity and selectivity of the sensor.

In the present work, a highly sensitive and selective ECL biosensor for miRNA-21 was proposed with a newly designed DNA functionalized N-CQD. Here, graphene oxide (GO)/Au nanocomposites were used for the immobilization of hairpin probe2 (HP2) and to promote electric transmission. The stable N-CQDs could produce strong ECL signals with high sensitivity, while the hairpin probe1 (HP1), which was linked to N-CQDs via the amide bond, was responsible for the high selectivity of this method (Scheme 1). The HP1-QDs were incubated with the assistant probe and the target miRNA to form the Y junction structure. HP1 contains three functional regions: a miRNA-binding domain that is complementary to the sequence of the target miRNA-21 (the yellow region), a complementary domain of assistant probes that acts as the recognition sequence for the nicking enzyme Nb.BbvCI (the green region), and a complementary domain of HP2 (the red region). The nicking enzyme Nb.BbvCI cleaved the Y junction on the cleavage site (5′-GC↓TGAGG-3′), bringing about the release of the target miRNA, assistant DNA, and the generation of intermediate N-CQDs-DNA (S1). Meanwhile, the released target miRNA and assistant DNA hybridized with other HP1-QDs to initiate another recycling process to generate abundant S1, which was promising for signal amplification. After the completion of the nicking enzyme-assisted signal amplification (NESA), these intermediate sequences were further hybridized with HP2. The stem-loop structure was opened to form dsDNA immobilized on the GO/Au composite modified GCE surface through an Au-S bond. After construction of the dsDNA junction structure, the initial ECL intensity was enhanced by the N-CQDs. Thus, the quantitative detection of target miRNAs can be achieved by adjusting the ECL signal to the concentration of target miRNA. The nicking enzyme Nb.BbvCI-induced target RNA cycling and the

N-CQDs-based enhanced ECL with the co-reactant $S_2O_8^{2-}$ resulted in an ECL biosensor with an ultrasensitive response to the target miRNA.

2. Experimental

2.1. Materials and Reagents

6-mercapto-1-hexanol (MCH), N-hydroxy succinimide (NHS), N-(3-dimethylaminopropyl)-N'-ethylcarbodiimide hydrochloride (EDC) and tri-(2-carboxyethyl) phosphine hydrochloride (TCEP) were purchased from Sigma-Aldrich Chemical Co. (U.S.A.). Diethy pyrocarbonate (DEPC) was provided by Sangon Biotech (Shanghai, China). Nb.BbvCI nicking enzyme and 10×NEbuffer (50 mM KAc, 20 mM Tris acetate buffer, 10 mM magnesium acetate, 100 μg/μL BSA, pH 7.9 at 25 °C) were obtained from New England Biolabs (USA) and used without further purification. The DNA sequence was obtained from Sangon Biotech (Shanghai, China) and used as Received. All miRNA sequences were from Genepharma (Shanghai, China) with HPLC purification. All DNA sequence information are as following.

Hairpin Probe1 (HP1): 5'-CTGCAACATCAGCTGAGGGGAAGAGATCAACACTTGCAGTTTT -$(CH_2)_6$-3'-NH_2

Hairpin Probe2 (HP2): 5'-AACGCAAGTGTTGATCTCTTCCCCTCAGCGTT-$(CH_2)_6$-3'-SH

Assistant Probe (AP): 5'-CCTCAGCTAGTCTGATAAGCTA-3'

Target miRNA-21: 5'-UAGCUUAUCAGACUGAUGUUGA-3'

Single base mismatched miRNA (SM miRNA-21): 5'-UAGCUUAUCACACUGAUGUUGA-3'

Three base mismatched miRNA (TM miRNA-21): 5'-UCGCUUAUCACACUGAUGUCGA-3'

miRNA-155: 5'-UAGCAGCACGUAAAUAUUGGCG-3'

miRNA-101: 5'-UACAGUACUGUGAUAACUGAA-3'

Buffers involved in this work were as follows: 10 mM Tris−HCl (pH 7.4) containing 1.0 mM EDTA, 1.0 M NaCl, and 1.0 mM TCEP was used as probe immobilization buffer; 10 mM Tris-HCl, 1.0 mM EDTA, 0.1 M NaCl, 10 mM $MgCl_2$ (pH 7.4), was employed as

miRNA hybridization buffer; 10 mM Tris-HCl (pH 7.4) was used as washing buffer. Phosphate buffer solutions (0.1 M PBS) were prepared with $Na_2HPO_4 \cdot 12H_2O$ and $NaH_2PO_4 \cdot 2H_2O$, containing 0.1 M $K_2S_2O_8$, 0.1 M NaCl and 0.1 M KCl served as the electrolyte in ECL analysis (pH 7.4). To avoid the effect of RNase on the stability of miRNAs, all centrifuge tubes (Axygen, USA) and tips (Axygen, USA) were autoclaved, and the redistilled deionized water treated with DEPC was used throughout this work.

2.2. Apparatus

The ECL measurements were performed on a model MPI-E electrochemiluminescence analyzer (Xi′An Remax Co. Ltd., China) with the photomultiplier tube set at 800 V and the potential scan was from 0 V to -1.6V at a scan rate of 0.3 V/s. Cyclic voltammetry (CV) was performed with a CHI660D electrochemical workstation (Shanghai Chenhua Instrument, China) by scanning the potential from -0.2 to 0.6 V at a scan rate of 100 mV/s in the electrolyte containing 5 mM of $Fe(CN)_6^{4-/3-}$ and 0.1 M of KCl. Electrochemical impedance spectroscopy (EIS) was performed with an Auto lab electrochemical analyzer (EcoChemie, Netherlands) in 5 mM $K_3Fe(CN)_6/K_4Fe(CN)_6$ (0.1 M KCl) as the supporting electrolyte at a bias potential of 0.18 V, within the frequency range of 0.1–100 kHz. All experiments were proposed in a conventional three-electrode system: a platinum wire was the counter electrode, Ag/AgCl (saturated KCl) was the reference electrode, and the modified glassy carbon electrode (GCE, Φ = 4 mm) was working electrode.

UV-vis absorption spectra were carried out on a UV-3600 UV-vis-NIR photospectrometer (Shimadzu Co., Japan). Fluorescence spectra were obtained on a RF-540 spectrophotometer (Shimadzu Co., Japan). Transmission electron microscopy (TEM) and high resolution transmission electron microscopy (HRTEM) images were performed with a model 2000 instrument (JEOL Co. Japan). X-ray photoelectron spectroscopy (XPS) analysis was carried out with a VG Scientific ESCALAB 250 spectrometer. The Fourier transform infrared spectroscopy (FT-IR) was recorded on a

Bruker VECTOR22 spectrometer.

2.3. Synthesis of nitrogen-doped carbon QDs (N-C QDs)

The synthesis was similar to that described in the literature with some modification (Tang et al., 2014). The synthesis of N-CQDs was carried out in a microwave synthesizer (CEM Discovery, CEM Inc. USA). First, 0.20 g of citric acid and 0.083 g of melamine were dispersed into 5 mL of the redistilled deionized water to ultrasound for 30 min. Then, put into a 10 mL quartz microwave reaction vessel, and transferred into the microwave synthesizer. The maximum power setting was set as 100 W and the pressure cut off limit was 200 psi. The temperature was ramped to 160 °C, and heated for 20 min. When cooled down to room temperature, the large particles were removed by filtration using a 0.22 μm filter membrane and then centrifuged at 8000 rpm for 15 min. The obtained milky N-C QDs solution were further dialyzed in a dialysis bag (retained molecular weight: 1000 Da) for five days to remove the excessive precursors.

2.4. Preparation and modification of GO/AuNPs composites

The GO/AuNPs composites were prepared by the reduction of gold (III) complex with sodium citrate (GilGoncalves et al., 2009). Typically, 300 μL of 1% $HAuCl_4$ solution was added into 4 mL of 0.1 mg/mL GO solution with stirring for 30 min at room temperature. Then 400 μL of 42 mM sodium citrate was added dropwise into the above mixture under vigorous stirring at 100 °C for 60 min. The resulting mixture was centrifuged (15 min, 5000 rpm), and the resultant composite was washed with distilled water to remove the free gold nanoparticles.

2.5. Preparation of N-C QDs —Hairpin probe1 (HP1)

70 μL of HP1 (10 μM, in 10 mM pH 7.4 Tris−HCl buffer containing 1.0 M NaCl) was heated at 95 °C for 10 min and then cooled to room temperature. The –COOH groups of the N-C QDs were activated by thoroughly mixing them (100 μL) in an aqueous solution of EDC (20 mg/mL) and NHS (10 mg/mL) and then incubating for 1 h at 37°C. Subsequently, the annealed amino-functionalized HP1(10 μM, 20 μL) was

added to the activated N-C QDs aqueous solution, and then the whole solution was incubated for 1 h at 37 °C to link N-C QDs and HP1 through covalent coupling by amide bond formation. The above stock solution was stored in the dark at 4 °C until use. Followed by centrifugation and wash three times at 15000 rpm for 15 min at 4 °C to remove excess HP1, the QDs−HP1 were obtained, which were dispersed in the Tris-HCl (10 mM, pH 7.4) buffer and stored in the refrigerator at 4 °C when not in use.

2.6. Nicking Enzymes Nb.BbvCI Mediated Signal Amplification (NESA)

The NESA was carried out by incubating the mixture of N-C QDs−HP1(1 μM), assistant DNA (1 μM), a series of various concentration of the target miRNA-21 and Nb.BbvCI nicking enzyme (8 U) in 10 × NEB buffer at 37 °C for 55 min to produce massive intermediate sequences (S1). Finally, the mixtures were heated to 80 °C and kept for 20 min to deactivate the Nb.BbvCI nicking enzyme, followed by cooling down to room temperature and the resulted products were stored at 4 °C.

2.7. Fabrication of the miRNA Biosensor

Prior to use, the Hairpin probe2 (HP2) were denatured for 2 min at 95 °C and slowly cooled to room temperature to form stem-loop structures. Before modification, the GCE was polished with 0.3 and 0.05 μm alumina slurry and then sonicated in water, ethanol, and water for 2 min each to obtain a mirror like surface, and then dried by nitrogen. The fabrication process for the ECL biosensor was demonstrated in Scheme 1B. At first, 10 μL of GO/Au composites were dropped onto the electrode surface to form a uniform film by drying in air at room temperature. Next,10 μL of probe immobilization buffer (10 mM Tris-HCl, 1.0 mM EDTA, 1.0 M NaCl, 1.0 mM TCEP, pH 7.4) containing 1 μM of thiol-modified HP2 was attached onto the GO/Au layer surface at 4°C damp environment for overnight, resulting in assembling HP2 on the modified electrode via Au −S affinity. After that, the modified electrode was rinsed with washing buffer and blocked with 10 μL of MCH (10 mM) for 60 min at 37 °C to prevent nonspecific adsorption followed by washing with washing buffer. Ultimately, the obtained biosensor

of MCH/Hairpin probe2/GO-Au/GCE was stored at 4 °C until use.

2.8. Measurement Procedure

The modified electrode was then incubated with the mixture of the reaction product of NESA for 1 h at 37 °C to capture the intermediate sequences (S1) on the modified electrodes by their complementary sequences (HP2) through DNA hybridizations. After incubation, the biosensor was rinsed with washing buffer to remove the unbound intermediate sequences. The obtained electrodes were detected with the MPI-E ECL analyzer in PBS (0.1 M, pH 7.4) at room temperature. The results displayed that the ECL signal increased with the increasing concentration of miRNA-21.

3. Results and discussion

3.1. *Characterizations of GO, GO/AuNP and N-CQD*

The synthesized GO and GO/AuNP hybrids were characterized using TEM. As shown in Figure 1A, the restacked parts and wrinkles can also be seen. AuNPs were uniformly distributed on the surface of the GO (Figure 1B), which was beneficial for HP2 attachment and improved the electronic transfer rate. The morphology and structure of the as-prepared N-CQDs are shown in Figure 1C. The N-CQD show uniform spherical shapes with an average size of 4.5 nm, as estimated from the TEM image (Figure 1C), indicating that the as-synthesized N-CQDs were well monodispersed and uniform in size. The lattice spacing in the HRTEM image is approximately 0.22 nm, which is consistent with (002) planes of graphitic carbon (Figure 1D, inset) (Baker et al., 2010; Tetsuka et al., 2012).

The surface composition and elemental analyses of the N-CQDs were performed by XPS. The full range XPS analysis (Figure 3A) of the resultant N-CQDs clearly showed three peaks at 285.2, 399.5, and 532.2 eV corresponding to C1s, N1s, and O1s, respectively. The spectrum of C1s in the N-CQDs (Figure 3B) can be deconvoluted into

several single peaks that correspond to sp^2C (283.1 eV), sp^3C (284.0 eV), C-O (286.9 eV), and C=N/C=O (287.8 eV) functional groups, which was consistent with the FTIR (Li et al., 2013). The N1s peaks at 397.6, 398.5, and 399.2 eV shown in Figure 2B indicated that nitrogen existed mostly in the form of C-N-C, $N-(C)_3$ and N-H, respectively (Zhang et al., 2014), implying that N was partly doped into the CQDs. The O1s spectrum (Figure 3D) showed two peaks at 530.4 and 531.6 eV, which were attributed to C=O, C-OH/C-O-C, respectively.

3.2. *ECL mechanism of N-CQD*

Figure 3A shows the relationship between the ECL curve (b) and the CV curve (a) for N-C QDs. The ECL peak from the N-C QDs/$K_2S_2O_8$ system appeared around −1.56 V with an onset potential of −0.8 V during the cyclic scanning between 0 and −1.6 V, indicating that the co-reactant $K_2S_2O_8$ enhanced the ECL emission of N-C QDs significantly. Based on the results described above, a possible ECL mechanism for the N-C QDs is as follows: theoretically, N-C QDs could be reduced to negatively charged $(N\text{-}C)^{\bullet-}$ radicals under the potential negative scanning. The reduction of $S_2O_8^{2-}$ (the co-reactant) generates a strong oxidizing agent, $SO_4^{\bullet-}$ radicals, which accept an electron from the anion $(N\text{-}C)^{\bullet-}$ to form excited state species (N-C*). N-C* species generate ECL emission when returned to their ground state. The ECL behavior of N-C QD/$K_2S_2O_8$ is similar to that of other nanoparticle systems, such as CdSe QDs.

Figure 3B shows a good ECL stability of N-C QDs/GCE under continuous 600 s of CV sweeps. Moreover, no obvious change in the ECL intensity was observed after storage for 2 months. This ECL emission stability indicates that the N-C QDs is a promising nanomaterial to construct ECL-based biosensors.

3.3. *Feasibility of electrochemiluminescence biosensor*

CVs were performed to characterize the surface assembly process of the electrodes. As shown in Figure 3C, the bare GCE exhibited a well-defined redox peak of

$[Fe(CN)_6]^{3-/4-}$ (curve a). It is obvious that the peak current was the highest on the GO/Au modified electrode because the conductive AuNPs could accelerate the electron transfer. After the immobilization of HP2, MCH layer by layer in Figure 3C (c, d), the peak currents decreased gradually. This could be attributed to the fact that HP2 and MCH can hinder the diffusion of ferricyanide toward the electrode surface. As expected, when the modified electrode was incubated with intermediate sequences (S1) (generated by the NESA process), the peak current further decreased curve (e) because of the electrostatic repulsion of $[Fe(CN)_6]^{3-/4-}$ from the electrode surface by the negative charges on the DNA strands. Therefore, the above results demonstrated that each layer was successfully modified on the electrode.

Electrochemical impedance spectra (EIS) were used to further characterize the electrode modification steps. As shown in Figure 3D, the Nyquist plots were fitted by the Randles equivalent circuit (Figure 3D, inset), where R_s is the solution resistance, C_d is the capacitance, R_{ct} is the charge transfer resistance, and Z_W is the Warburg impedance. The R_{ct} of the electrode is equal to the semicircle diameter of the Nyquist diagram. The bare GCE displayed a small semicircle (curve a), indicating good electrical conductivity of the interface. After GO/Au were modified on the electrode surface, the resistance decreased (curve b). This suggested that GO/Au could improve the conductivity and accelerate the electron transfer. With the immobilization of HP2, and MCH the R_{et} value was further increased (curves c and d). These increases could be explained as the electrostatic repulsion effect between the negatively charged phosphoric acid backbone of oligonucleotides and $[Fe(CN)_6]^{3-/4-}$. After incubation with intermediate sequences (S1), the semicircle further increased (curve h), which could be attributed to the fact that intermediate sequences further hindered the electron transfer. These results were in agreement with the CV results.

3.5. *ECL Analysis of the miRNA-21 Biosensor*

Under the optimized experimental conditions (supporting information), the analytical performance of the proposed biosensor for detecting miR-21 at various concentrations is shown in Figure 4. The relationship between the ECL response and miR-21 concentration is shown in Figure 4A. The ECL signal increased gradually with increasing miR-21 concentrations (curves a–g), and a linear range for miR-21 was obtained from 10 aM to 10^4 fM with a detection limit of 10 aM (S/N=3) (Figure 4B). The linear relationship could be represented as I = 981.07 logc + 3471.3, with a correlation coefficient of 0.9980, where I stands for the ECL intensity and c stands for the concentration of miR-21. This showed the efficacy of the proposed biosensor for the sensitive detection of miR-21, which was attributed to the application of nicking enzyme assisted target recycling and the stable ECL intensity of N-CQDs. In addition, compared with other miR-21 biosensor methods (Table S1), the proposed ECL biosensor exhibited higher sensitivity with a lower detection limit.

3.6. *Stability, reproducibility and specificity of the biosensor*

The stability of the ECL biosensor was evaluated under continuous scanning for 20 cycles in 0.1 M PBS (containing 0.1 M $K_2S_2O_8$, pH 7.4) at 10 fM of miR-21. As shown in Figure 4C, there was no significant change of the ECL response with a relative standard deviation (RSD) of 1.12%. There are two possible reasons for the observed stability: Firstly, the GO/Au composites provided good bioactivity, superior conductivity, and increased loading of HP2 chains, which could accelerate efficient electron transfer and increase the available chances of the chains. Simultaneously, the high efficiency of the nicking enzyme induced target recycling and resulted in a particular luminescence superiority of N-CQD, which remarkably increased the ECL intensity and stability.

The reproducibility of the proposed biosensor was also examined by using 10 fM of miR-21 for five reduplicate measurements in the intra-assay and inter-assay. The RSD values were 3.2% and 5.4%, respectively, which demonstrated that the reproducibility of the proposed biosensor for detecting miR-21 was acceptable.

To investigate the selectivity and specificity of the proposed biosensors, as depicted in Figure 4D, the selective recognition of miR-21 by the biosensor was explored by using 100 pM of miR-155, 100 pM of miR-101, 100 pM of single-base mismatched miR-21 (SM miR-21), and 100 pM of two-base mismatched miR-21 (TM miR-21) to replace 10 fM of miR-21. The results showed that the ECL signal of the biosensors had negligible intensity compared with the blank incubated with miR-155 and miR-101. The results showed that the ECL signals from SM miR-21 and TM miR-21 were slightly increased compared with the blank. Nevertheless, 10 fM miR-21 and miR-21 (10 fM) with interfering substances exhibited a much stronger response than the blank, suggesting that only the perfectly matched sequence could trigger signal amplification strategies, and the designed scheme had good selectivity toward miR-21 compared with control RNA.

4. CONCLUSIONS

The proposed ECL biosensor was constructed for the detection of miRNAs based on target cycling amplification with a novel nicking enzyme, Nb.BbvCI, and DNA functionalized N-CQDs enhancement. The newly designed nicking enzyme-triggered cycling reaction achieved promising amplification intermediate sequences and good efficiency under optimal conditions. In addition, with the help of the high ECL intensity provided by the N-CQDs, the present assay can provide a wide linear range and satisfactory sensitivity for miR-21 detection.

Acknowledgements

This work was supported by the National Natural Science Foundation of China (Grant Nos. 21427807, 21575001), Natural Science Foundation of Anhui Province (1508085MB37).

References

Baker, S. N., Baker, G. A., 2010. Angew. Chem. Int. Ed. 49, 6726–6744.

Bernstein, E., Caudy, A. A., Hammond, S. M., Hannon, G. J., 2001. Nature 409, 363-366.

Bartel, D. P., 2009. Cell 136, 215-233.

Dong, Y. Q., Pang, H. C., Yang, H. B., Guo, C. X., Shao, J. W., Chi, Y. W., Li, C. M., Yu, T., 2013. Angew. Chem. Int. Ed. 52, 7800-7804.

Goncalves, G., Marques, P. A. A. P., Granadeiro, C. M., Nogueira, H. I. S., Singh, M. K., Gracio, J., 2009. Chem. Mater. 21, 4796-4802.

Han,Y. Z., Tang, D., Yang, Y. M., Li, C. X., Kong, W. Q., Huang, H., Liu, Y., Kang, Z. H., 2015. Nanoscale 7, 5955-5962.

Hu, S. L., Trinchi, A., Atkin, P., Cole, I., 2015. Angew. Chem. Int. Ed. 127, 3013-3017.

Huang, R. C., Chiu, W. J., Li, Y. J., Huang, C. C., 2014. ACS Appl. Mater. Interfaces 6, 21780-21787.

Hébert, S. S., Strooper, B. D., 2007. Science 317, 1179-1180.

Hu, L. Z., Xu, G. B., 2010. Chem.Soc. Rev. 39, 3275-3304.

Hesari, M., Swanick, K. N., Lu, J. S., Whyte, R.,Wang, S. N., Ding, Z. F., 2015. J. Am. Chem. Soc. 137, 11266-11269.

Hu, X. W., Mao, C. J., Song, J. M., Niu, H. L., Zhang, S. Y., Huang, H. P., 2013. Biosens. Bioelectron. 41, 372-378.

Han, C. P., Wang, R., Wang, K. Y., Xu, H. T., Sui, M. R., Li, J. J., Xu, K., 2016. Biosens. Bioelectron. 83, 229-236.

Jiang, K., Sun, S., Zhang, L., Wang, Y. H., Cai, C. Z., Lin, H. W., 2015. Appl. Mater. Interfaces 7, 23231-23238.

Kumar, V. B., Sheinberger, J., Porat, Z., Shav-Tal, Y., Gedanken, A., 2016. J. Mater. Chem. B 4, 2913-2920.

Kosaka, N., Iguchi, H., Ochiya, T., 2010. Cancer Sci. 101, 2087-2092.

Lim, S. Y., Shen, W., Gao, Z. Q., 2015. Chem. Soc. Rev. 44, 362-381.

Li, W., Zhang, Z. H., Kong, B., Feng, S. S., Wang, J. X., Wang, L. Z., Yang, J. P., Zhang, F., Wu, P. Y., Zhao, D. Y., 2013. Angew. Chem. Int. Ed. 52, 8151-8155.

Mueller, M. L., Yan, X., McGuire, J. A., Li, L. S., 2010. Nano Lett. 10, 2679-2682.

Martinsa, N. C. T., Ângeloa, J., Girãob, V. A., Trindadeb, T., Andradea, L., Mendesa, A. 2016. Applied Catalysis B:Environmental 193, 67–74.

Miao, W. J., 2008. Chem. Rev. 108, 2506-2553.

Tetsuka, H., sahi, R., Nagoya, A., Okamoto, K., Tajima, I., Ohta, R., Okamoto, A., 2012. Adv. Mater. 24, 5333-5338.

Tang, J., Zhang, Y. Y., Kong, B., Wang, Y. C., Da, P. M., Li, J., Elzatahry, A. A., Zhao, D. Y., Gong, X. G., Zheng, G. F., 2014. Nano Lett. 14, 2702-2708.

Volinia, S., Calin, G. A., Liu, C. G., Ambs, S., Cimmino, A., Petrocca, F., Visone, R., Iorio, M., Roldo, C., Ferracin, M., 2006. Proc. Natl. Acad. Sci. U. S. A. 103, 2257-2261.

Wang, N., Wang, Y. T., Guo, T. T., Yang, T., Chen, M. L., Wang, J. H., 2016. Biosens. Bioelectron. 85, 68-75.

Wu, Z. L., Zhang, P., Gao, M. X., Liu, C. F., Wang, W., Lenga, F., Huang, C. Z., 2013. J. Mater. Chem. B 1, 2868-2873.

Wienholds, E., Kloosterman, W. P., Miska, E., Alvarez-Saavedra, E., Berezikov, E., de Bruijn, E., Horvitz, H. R., Kauppinen, S., Plasterk, R. H. A., 2005. Science 309, 310-311.

Xiong, C. Y., Liang, W. B., Wang, H. J., Zheng,Y. N., Zhuo, Y., Chai, Y. Q., Yuan, R., 2016. Chem. Commun. 52, 5589-5592.

Yan, X., Cui, X., Li, L.S., 2010. J. Am. Chem. Soc. 132, 5944-5945.

Yu, C. M., Li, X. Z., Zeng, F., Zheng, F. Y., Wu, S. Z., 2013. *Chem. Commun. 49*, 403-405.

Zhang, H. J., Chen, Y. L., Liang, M. J., Xu, L. F., Qi, S. D., Chen, H. L., Chen, X. G., 2014. Anal. Chem. 86, 9846-9852.

Zheng, L. Y., Chi, Y. W., Dong, Y. Q., Lin, J. P., Wang, B. B., 2009. J. Am. Chem. Soc. 131, 4564-4565.

Scheme1. Schematic diagrams of the sensor: (A) the nicking enzymes Nb.BbvCI Mediated signal amplification (NESA); (B) fabrication of the biosensor: (a) modifying GCE with GO/Au composite, (b) assembly of HP2, (c) incubation of MCH, (d) the forming of signal enhancer; (C) the ECL enhancement mechanism of the self-enhanced N-C QDs.

Figure 1. TEM image of (A) GO and (B) GO/AuNPs hybrids; (C) TEM image and (D) High-resolution TEM image of the N-CQD.

Figure 2. XPS spectra of the N-CQD. (A) Survey spectrum. (B) C1s spectrum. (C) N1s spectrum. (D) O1s spectrum.

Figure 3. (A) ECL intensity-potential curves (b) and Cyclicvoltammogram (a) of N-CQD. (B) Stability of the ECL signals of N-CQD scanning from 0 to -1.6 V in 0.1 mol L^{-1} PBS (pH 7.4) containing 0.1 mol L^{-1} $S_2O_8^{2-}$. (C) the curves of CVs and (D) EIS for the stepwise biosensor fabrication measured in 5.0 mM $[Fe(CN)_6]^{3-/4-}$ containing 0.1 M KCl and with the scan range of -0.2 to 0.6 V at the rate of 100 mV/s. (a) bare GCE, (b) GO-Au/GCE, (c) HP2/GO-Au/GCE, (d) MCH/HP2/GO-Au/GCE, (e) S1/MCH/HP2/GO-Au/GCE. The concentration of miRNA-21 is 10 fM.

Figure 4. (A) Cathodic ECL response of the designed biosensor in the presence of different concentrations of miRNA-21): (a) 10^{-2}, (b) 10^{-1}, (c) 1, (d) 10, (e) 10^2, (f) 10^3 and (g) 10^4 fM. (B) The corresponding calibration curve of the biosensor for miR-21 assay. The ECL signals were measured in 0.1 M PBS (pH 7.4) containing 0.1 M $K_2S_2O_8$ by scanning the potential from 0 to -1.6 V at a scanning rate of 300 mV/s. (C) Stability of the proposed ECL biosensor under a continuous cyclic potential scan for 20 cycles. (D) Selectivity of the proposed ECL biosensors with different targets: (a) blank, (b) 100 pM

miRNA-155, (c) 100 pM miR-101, (d) 100 pM SM miRNA-21, (e) 100 pM TM miRNA-21, (f) 10 fM miRNA-21, and (g) a mixture (containing 100 pM miRNA-155, 100 pM miRNA-101, 100 pM SM miRNA-21, 100 pM TM miRNA-21 and 10 fM miR-21).

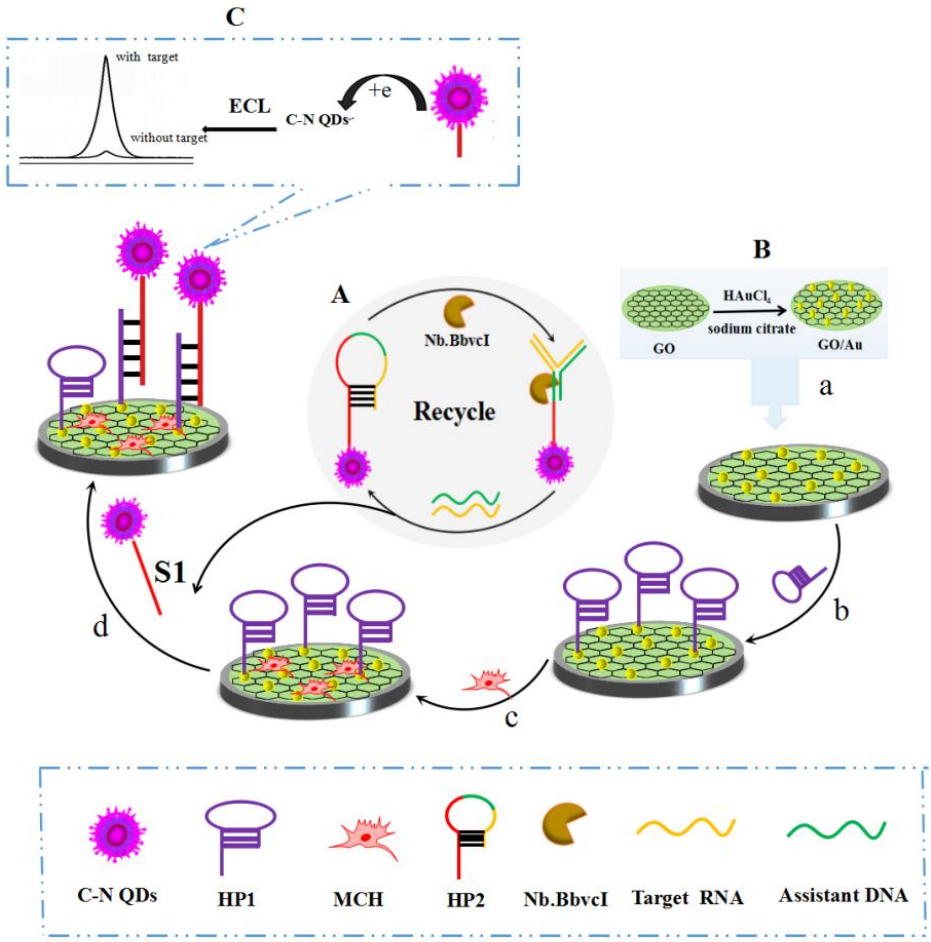

Scheme 1

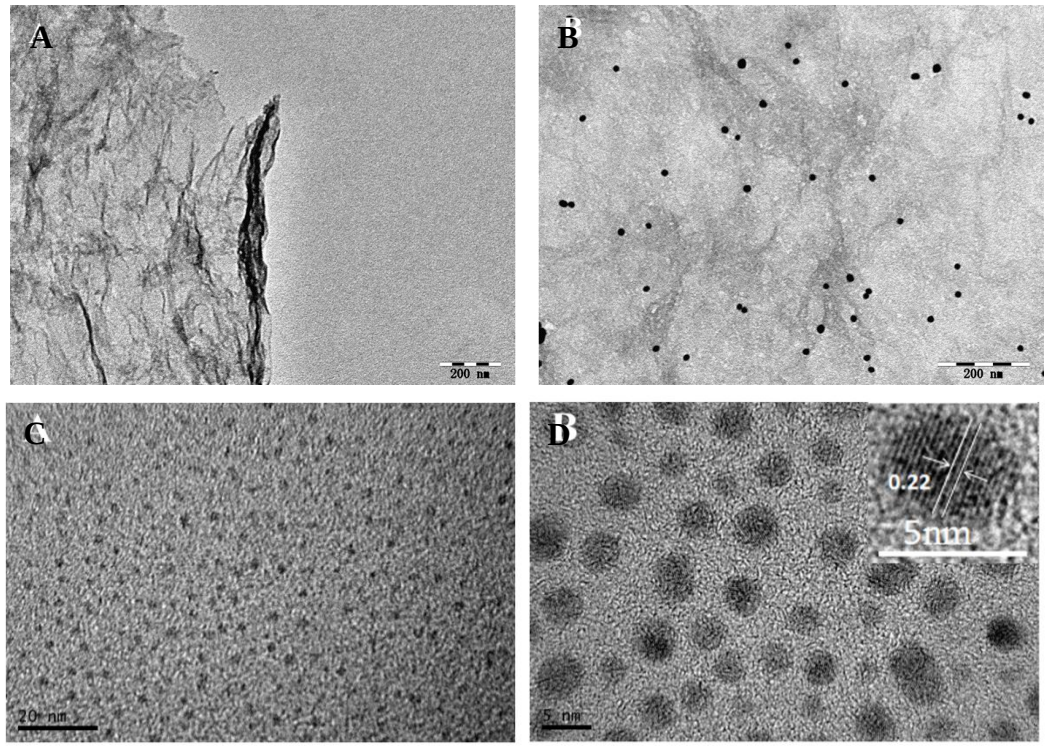

Figure 1

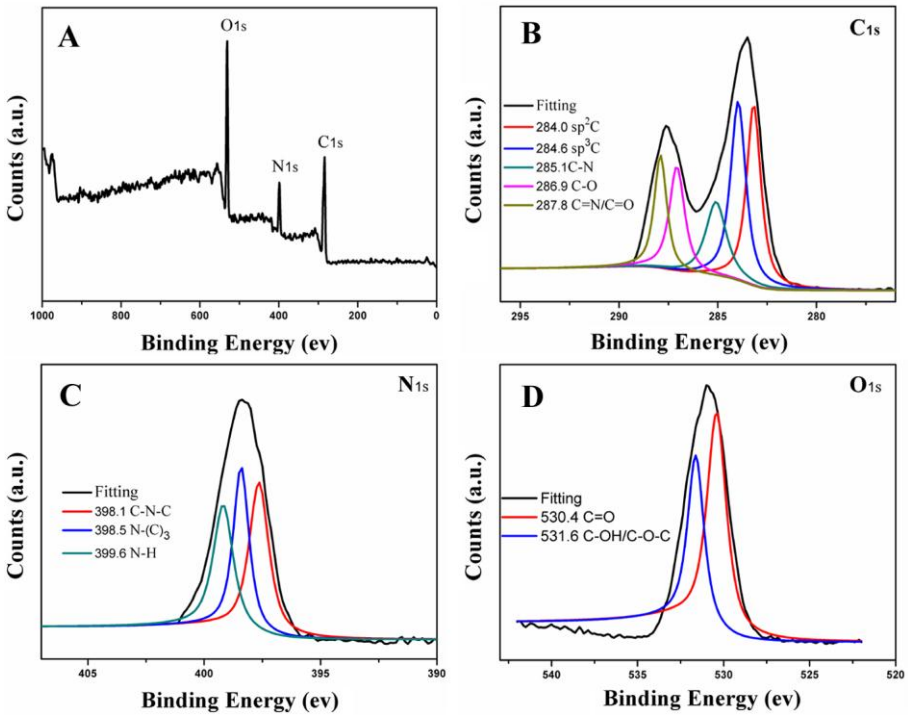

Figure 2

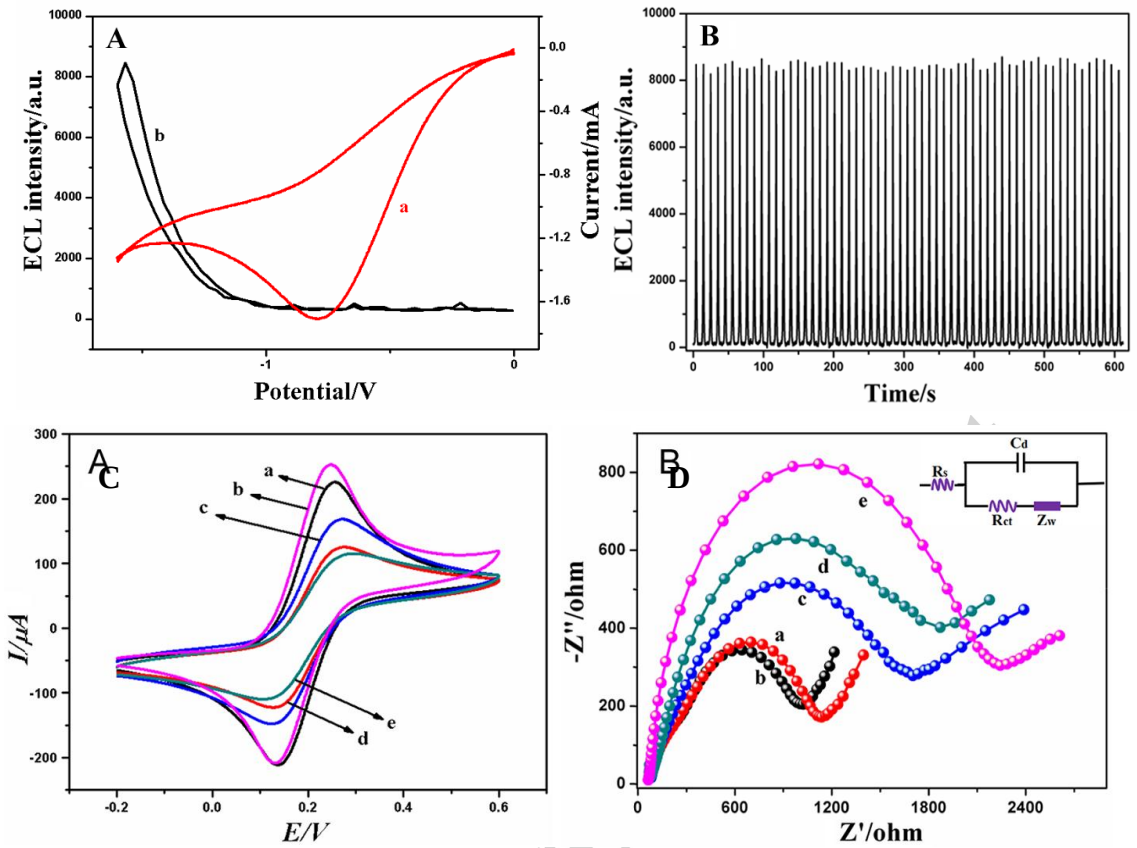

Figure 3

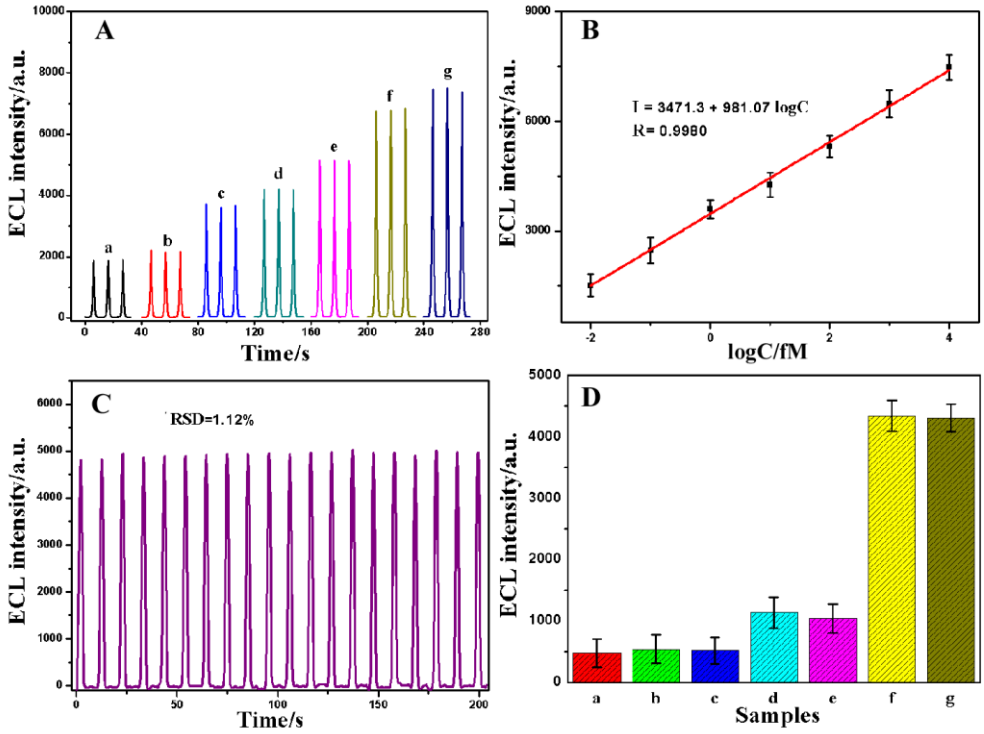

Figure 4

Highlights

- Uniform, water-soluble and nontoxic N-C QDs were firstly synthesized.
- DNA functionalized N-C QDs as signal enhancers to construct an ultrasensitive ECL biosensor to detect miRNA-21.
- Nicking enzymes (Nb.BbvCI) were utilized to trigger target cycling reaction to realize efficient signal amplification.